Chemistry and Ecology

Removal of Remazol Brilliant Violet-5R dye using periwinkle shells

Olugbenga Solomon Bello [a][b] & Mohd Azmier Ahmad [a]

[a] School of Chemical Engineering, Universiti Sains Malaysia, Penang, Malaysia

[b] Department of P/A Chemistry, Ladoke Akintola University of Technology, Ogbomoso, Nigeria

Available online: 17 Aug 2011

PLEASE SCROLL DOWN FOR ARTICLE

Removal of Remazol Brilliant Violet-5R dye using periwinkle shells

Olugbenga Solomon Bello[a,b]* and Mohd Azmier Ahmad[a]

[a]*School of Chemical Engineering, Universiti Sains Malaysia, Penang, Malaysia;* [b]*Department of P/A Chemistry, Ladoke Akintola University of Technology, Ogbomoso, Nigeria*

The purpose of this research is to obtain optimal processing conditions for the adsorption of Remazol Brilliant Violet-5R (RBV-5R) dye onto activated carbon prepared from periwinkle shells (PSAC) by chemical activation with KOH using response surface methodology. Central composite design (CCD) was used to determine the effects of three preparation variables; CO_2 activation temperature, CO_2 activation time and KOH:char impregnation ratio (IR) on two responses; percentage RBV-5R dye removal and PSAC yield. Based on the CCD, two quadratic models were developed for percentage RBV-5R dye removal and PSAC yield, respectively. The most influential factor on each experimental design response was identified from the analysis of variance (ANOVA). The optimum conditions for the adsorption of RBV-5R dye onto PSAC were CO_2 activation temperature of 811 °C, CO_2 activation time of 1.70 h and IR of 3.0, resulting in 81.28% RBV-5R dye removal and 28.18% PSAC yield. PSAC prepared under optimum conditions was mesoporous with a Brunauer–Emmett–Teller surface area of $1894 \, m^2 \cdot g^{-1}$, total pore volume of $1.107 \, cm^3 \cdot g^{-1}$ and average pore diameter of 2.32 nm. The surface morphology and functional groups of the activated carbon were respectively determined from the scanning electron microscopy and Fourier transform infrared analysis.

Keywords: periwinkle shell activated carbon; adsorption; central composite design; dye; responses

1. Introduction

Water pollution is one of the most undesirable environmental problems in the world that requires urgent solution. Textile industries produce a lot of wastewater, which contains different contaminants, including acidic or caustic dissolved solids, toxic compounds and different type of dyes. Many of the organic dyes are hazardous and may affect aquatic life causing various diseases and disorders [1]. Synthetic dyes are used extensively for textile dyeing and other industrial applications. Total world colourant production is estimated to be ∼800,000 ton·year^{-1}. More than 10,000 dyes are commercially available and at least 10% of the dyestuff used enters the environment as wastes [2]. These industrial effluents are toxic and are characterised by high chemical oxygen demands (CODs)/biological oxygen demands (BODs), suspended solids and intense colour [3]. Furthermore, these coloured molecules are highly conjugated and can be extremely injurious to the life [4]. Synthetic dyes, classified by their chromophores, have different and stable chemical

---

*Corresponding author. Email: osbello@yahoo.com

structures to meet various colouring requirements and they are often difficult to degrade and/or remove using conventional physical and chemical processes [5,6]. Remazol Brilliant Violet Reactive (RBV-5R) is one of the most important dyes in the textile industry. It is frequently used as a starting material in the production of polymeric dyes. RBV-5R is an anthracene derivative and represents an important class of toxic and recalcitrant organic pollutants.

Marine snails in general are part of the family Gastropoda. They are found in oceans all over the world. The major species available in the lagoon and mudflats of Nigeria's Niger Delta, between Calabar in the east and Badagry in the west, are *Typanostonus* spp. and *Pachmellania* spp. Over the years, lots of periwinkle shells have accumulated in many parts of the country such as Bori, Western Ijaw, Burutu, Agoro, Ogalaga and Lotugbene, thereby causing a serious environmental challenge. In this study, periwinkle (*Typanotonus fuscatus*), which is abundant in the Niger Delta in Nigeria along the mangrove intertidal wetland within the upper part of Bonny River system adjoining a densely populated municipal environment, was used for activated carbon preparation. Periwinkles are usually 1.3–2.5 cm in height, and their colouration varies from grey to black. The shell is fairly heavy and solid. To make better use of this abundant waste, it was used in the preparation of activated carbon. Conversion of periwinkle shell (PS) to activated carbon serves a dual purpose. First, unwanted waste is converted to useful, value-added adsorbent and second, the use of PS as a potential source of adsorbent contributes to solving wastewater treatment problems in Nigeria. However, there are limited studies reported on the utilisation of PS, especially on conversion of PS into activated carbon. The most important characteristic of activated carbon is its adsorption performance, which is highly influenced by the preparation conditions that affect the pore development and surface characteristics of the activated carbon produced. Therefore, the challenge in activated carbon production is to produce specific carbons that are suitable for certain applications.

The experimental design technique is a very useful tool for this purpose because it provides statistical models that help in understanding interactions among parameters that have been optimised [6]. Response surface methodology (RSM) has been found to be a useful tool in studying the interactions of two or more variables [7,8]. Optimisation of experimental conditions using RSM has been widely applied in various processes. Some previous studies applying RSM in the preparation of activated carbons used precursors such as biochar [9], olive-waste cakes [10], Luscar char [11] and Turkish lignite [8]. To the best of our knowledge, there has been no study on the preparation of activated carbon from PS by physiochemical activation for adsorption of RBV-5R reactive dye from aqueous solutions using the RSM approach. Therefore, the focus of this research was to carry out a statistical optimisation to determine the optimum preparation conditions for activated carbon derived from PS, which gave high activated carbon yield and high RBV-5R reactive dye removal from aqueous solutions, because these data are required as the starting point for scaling-up the laboratory results to pilot-plant or full-scale levels [12]. A central composite design (CCD) was selected to simultaneously study the effects of three activated carbon preparation variables (CO_2 activation temperature, CO_2 activation time and impregnation ratio, IR) on two responses. Empirical models correlating RBV-5R reactive dye removal and the activated carbon yield with the three variables were then developed. The PS-based activated carbon prepared under optimum conditions was further characterised to determine its physical and chemical characteristics.

2. Material and methods

2.1. *Remazol Brilliant Violet 5R dye (RBV-5R)*

Remazol Brilliant Violet- 5R reactive dye supplied by Sigma-Aldrich (M) Sdn Bhd, Malaysia was used as an adsorbate. Deionised water was used to prepare all reagents and solutions.

2.2. *Preparation of periwinkle shell-based activated carbon (PSAC)*

PS was washed with water and subsequently dried at 105 °C for 24 h to remove moisture content. The dried PS was ground and sieved to a particle size of 1–2 mm before loading it into a stainless steel vertical tubular reactor placed in a tube furnace. A carbonisation step was carried out at 400 °C for 30 min under nitrogen (99.99%) flow at flow rate of 150 mL·min^{-1}. The char produced was mixed with KOH pellets at different impregnation ratio (IR), calculated using Equation (1):

$$\text{Impregnation ratio (I.R)} = \frac{W_{KOH}}{W_{Char}} \tag{1}$$

where W_{KOH} is the dry weight (g) of KOH pellets and W_{Char} is the dry weight (g) of char. Deionised water was then added to dissolve all the KOH pellets. The activation step was carried out using a similar reactor as in carbonisation step. Once the final activation temperature was reached, the gas flow was switched from nitrogen to CO_2 at a flow rate of 150 mL·min^{-1} for 2 h. The activated product was then cooled to room temperature under nitrogen flow. The sample was washed with hydrochloric acid (0.1 M). Thereafter it was washed with hot deionised water until the pH of the washed solution reached 6.5–7.

2.3. *Adsorption studies*

For batch adsorption studies, 0.2 g of PSAC were mixed with 100 mL aqueous dye solution of 100 mg·L^{-1} initial concentration in 20 sets of 250-mL Erlenmeyer flasks. The mixture was agitated at 120 rpm at 30 °C until equilibrium was reached. The concentration of RBV-5R dye solution was determined using a UV-visible spectrophotometer (UV-1800 Shimadzu, Japan) at a maximum wavelength of 577 nm. The percentage dye removal at equilibrium was calculated using Equation (2):

$$\text{Removal (\%)} = \frac{(C_o - C_e)}{C_0} \times 100 \tag{2}$$

where C_o and C_e are the liquid-phase dye concentrations at initial state and at equilibrium (mg·L^{-1}), respectively. The activated carbon yield was calculated using Equation (3):

$$\text{Yield (\%)} = \frac{W_c}{W_o} \times 100 \tag{3}$$

where W_c and W_o are the dry weight of final PSAC (g) and the dry weight of precursor (g), respectively.

2.4. *Design of experiment using CCD*

RSM is a collection of statistical and mathematical techniques that uses quantitative data from appropriate experiments to determine regression model equations and operating conditions which are useful for developing, improving and optimising processes [13]. In this work, a standard RSM design called CCD was applied to study the variables for preparing PSAC. This method reduces the number of experimental trials needed to evaluate multiple parameters and their interactions [14,15]. In this study, the preparation variables used were CO_2 activation temperature (x_1), CO_2 activation time (x_2) and KOH:char impregnation ratio (IR) (x_3). These three variables together with their respective ranges were chosen based on literature and preliminary studies are reported in Table 1.

Table 1. Independent variables and their coded levels for the CCD.

Variables (factors)	Code	Units	Coded variable levels				
			$-\alpha$	-1	0	$+1$	$+\alpha$
Activation temperature	x_1	(°C)	698.87	750.00	825.00	900.00	951.13
Activation time	x_2	(h)	0.32	1.00	2.00	3.00	3.68
Impregnation ratio (IR)	x_3	–	0.01	1.00	2.45	3.60	4.86

2.5. *Characterisation of PSAC*

The surface area, pore volume and average pore diameter of the PSAC were determined using a Micromeritics ASAP 2020 volumetric adsorption analyser. A 21-point analysis was carried out at 77 K to obtain the nitrogen adsorption isotherm. The surface area of the sample was determined using Brunauer–Emmett–Teller (BET) equation. The total pore volume was estimated to be the liquid volume of nitrogen at a relative pressure of 0.98. The surface morphology of the sample was examined using a scanning electron microscope (JEOL, JSM-6460 LV, Japan). Proximate analysis was carried out using thermo gravimetric analyser (Perkin-Elmer TGA7, USA) and Fourier transform infrared (FTIR) analysis was performed to determine the functional groups responsible for the adsorption of RBV-5R dye on PSAC.

3. Results and discussion

3.1. *Model fitting and statistical analysis*

The experimental data were analysed using a statistical software Design Expert software version 6.0.6 (STAT-EASE Inc., Minneapolis, USA) for regression analysis to fit the second-degree polynomial equation and also for the evaluation of the statistical significance of the equations developed [15,16].

3.1.1. *Development of regression model equation*

The complete design matrix together with the values of both the responses obtained from the experiment, are given in Table 2. Runs 15–20 at the centre point were conducted to determine the experimental error and the reproducibility of the data. RBV-5R dye removal was found to range from 30.54 to 92.48%, whereas the PSAC yield obtained ranged from 13.38 to 28.59%. According to the sequential model sum of squares, models were selected based on the highest order polynomials where the additional terms were significant and the models were not aliased. For both responses, RBV-5R dye removal and PSAC yield, the quadratic model was selected, as suggested by the software. The final empirical models in terms of coded factors after excluding the insignificant terms for RBV-5R dye removal (Y_1) and PSAC yield (Y_2) are shown in Equations (4) and (5), respectively.

$$\% \text{ RBV-5R dye removal } (Y_1) = 45.48 + 4.61x_1 + 2.52x_2 + 0.43x_3 - 3.78x_1^2 - 2.52x_2^2$$
$$- 0.73x_3^2 - 3.83x_1x_2 - -0.68x_1x_3 + 0.42x_2x_3 \quad (4)$$

$$\% \text{ PSAC yield } (Y_2) = 36.24 - 5.23x_1 - 2.23x_2 - 0.26x_3 + 0.54x_1^2 - 0.061x_2^2$$
$$+ 0.19x_3^2 + 0.59x_1x_2 + 0.026x_1x_3 - 0.20x_2x_3 \quad (5)$$

Table 2. Experimental design matrix for preparation of PSAC.

| Run | Level | | | PSAC preparation variable | | | RBV-5R removal, Y_1 (%) | PSAC yield Y_2 (%) |
				Activation temperature, x_1 (°C)	Activation time, x_2 (h)	IR, x_3		
1	−1	−1	−1	750.00	1.00	1.00	30.54	26.34
2	+1	−1	−1	900.00	1.00	1.00	33.24	23.05
3	−1	+1	−1	750.00	3.00	1.00	39.78	22.45
4	+1	+1	−1	900.00	3.00	1.00	45.89	16.56
5	−1	−1	+1	750.00	1.00	3.60	51.87	17.57
6	+1	−1	+1	900.00	1.00	3.60	61.56	17.09
7	−1	+1	+1	750.00	3.00	3.60	76.88	17.31
8	+1	+1	+1	900.00	3.00	3.60	69.53	13.38
9	−1.682	0	0	698.87	2.00	2.45	74.87	25.72
10	+1.682	0	0	951.13	2.00	2.45	87.16	18.56
11	0	−1.682	0	825.00	0.32	2.45	82.53	23.51
12	0	+1.682	0	825.00	3.68	2.45	90.84	17.84
13	0	0	−1.682	825.00	2.00	0.01	64.67	28.59
14	0	0	+1.682	825.00	2.00	4.86	87.68	17.56
15	0	0	0	825.00	2.00	2.45	92.48	23.31
16	0	0	0	825.00	2.00	2.45	82.84	22.18
17	0	0	0	825.00	2.00	2.45	82.56	22.75
18	0	0	0	825.00	2.00	2.45	83.55	23.01
19	0	0	0	825.00	2.00	2.45	82.54	22.02
20	0	0	0	825.00	2.00	2.45	83.40	22.11

The R^2 values for Equations (4) and (5) were 0.916 and 0.942, respectively. This indicated that 91.6 and 94.2% of the total variation in the percentage RBV-5R dye removal and PSAC yield, respectively, was attributed to the experimental variables studied. The quality of the model developed was evaluated based on the R^2 value. The R^2 values for the two models were considered relatively high, as they were both >0.9. This indicated that there was good agreement between the experimental and the predicted values for the responses obtained from these models. From the ANOVA, the response surface quadratic model for percentage RBV-5R dye removal and activated PSAC yield are shown in Table 3, the model F-value of 13.29 revealed that the model was significant. In this case, x_1, x_3, x_3^2 and $x_1 x_3$ were significant model terms, whereas x_2, x_1^2, x_2^2, $x_1 x_2$ and $x_2 x_3$ were all insignificant to the response.

From the ANOVA for the response surface quadratic model for PSAC yield presented in Table 4, the model F-value of 16.36 and Prob. > F of 0.0001 showed that the model was also significant.

Table 3. ANOVA for response surface quadratic model for RBV-5R dye removal using PSAC.

Source	Sum of squares	Degrees of freedom	Mean square	F-value	Prob. > F
Model	23271.23	9	1830.14	13.29	0.0001
x_1	3241.85	1	3241.85	18.18	0.001
x_2	420.60	1	320.60	2.11	0.2131
x_3	23.41	1	8524.96	42.32	<0.0001
x_1^2	44.2	1	44.20	0.21	0.6396
x_2^2	0.92	1	0.95	0.0013	0.7239
x_3^2	3721.20	1	3642.77	15.26	0.0178
$x_1 x_2$	412.77	1	286.42	2.74	0.2662
$x_1 x_3$	3540.55	1	3541.67	14.13	0.0031
$x_2 x_3$	648.33	1	672.55	3.81	0.0899
Residual	2164.41	10	207.41	–	–

Table 4. ANOVA for response surface quadratic model for PSAC yield.

Source	Sum of squares	Degrees of freedom	Mean square	F-value	Prob. $> F$
Model	328.40	9	328.40	16.36	0.0001
x_1	88.73	1	88.73	32.48	0.0002
x_2	16.21	1	16.21	5.88	0.0242
x_3	48.71	1	48.71	17.41	0.0016
x_1^2	121.23	1	121.23	46.16	<0.0001
x_2^2	38.43	1	38.43	14.24	0.0029
x_3^2	10.06	1	10.06	3.21	0.0646
$x_1 x_2$	0.054	1	0.054	0.024	0.07863
$x_1 x_3$	12.18	1	12.18	4.86	0.0531
$x_2 x_3$	12.18	1	12.18	4.86	0.0531
Residual	25.16	10	25.26	–	–

In this case, x_1, x_2, x_3, x_1^2 and x_2^2 were significant model terms whereas x_3^2 and the three interaction effects of $x_1 x_2$, $x_1 x_3$ and $x_2 x_3$ were negligible to the response.

3.1.2. *Percentage RBV-5R dye removal*

The percentage RBV-5R dye removal is shown in Figure 1. Percentage dye removal generally increases with an increase in activation temperature and IR. Higher CO_2 activation temperature and IR were favourable for enhancing the percentage RBV-5R dye removal as the increase in temperature and IR would cause the CO_2 to further gasify PSAC and accelerate the reaction rate, thus leading to increasing porosity and widening of the pores [17–19]. IR played a decisive role in the formation of pores because the KOH was dehydrated to K_2O, which further reacted with CO_2 produced by the water-shift reaction to give K_2CO_3. Intercalation of metallic
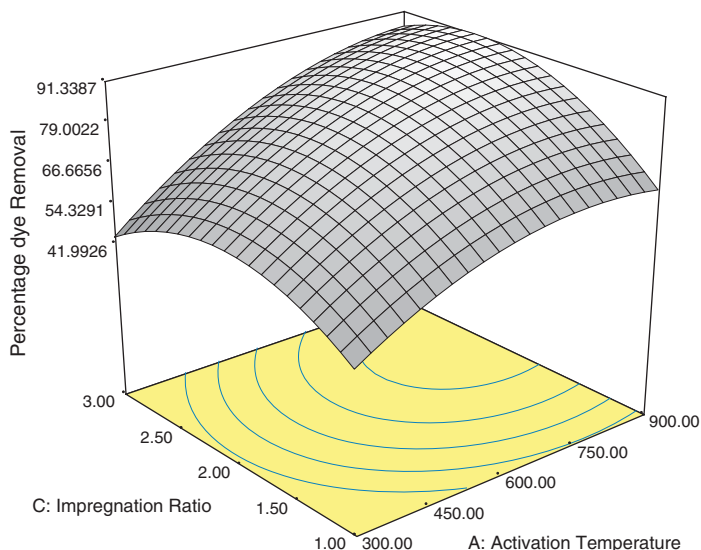

Figure 1.   Three-dimensional response surface plot of RBV-5R dye removal using PSAC (effect of activation temperature and IR, $t = 2$ h).

potassium, which was formed above 700 °C, appeared to be responsible for the drastic expansion of the carbon material and the creation of large surface area and high porosity, leading to the high percentage RBV-5R dye removal [18,19]. The results obtained revealed that activation time showed an insignificant effect on the percentage RBV-5R dye removal of the PSAC. This observation was in agreement with the study by Sudaryanto et al. [20] who reported that activation time had no significant effect on the pore structure of activated carbon produced from cassava peel, whereas the pore characteristics changed significantly with the activation temperature and also the KOH impregnation ratio. Gratuito et al. [21] stated that the duration of the activation had a significant effect on the development of the carbon porous networks; nevertheless, the activation time should just be enough to eliminate all the moisture and most of the volatile components in the precursor to cause the pores to develop. Because the end of the volatile evolution marked the formation of the basic pore structure, activation should be limited up to that point. The three variables studied were found to have synergistic effects on the percentage RBV-5R dye removal. This was expected as the increase in activation temperature and time would entail an opening and enlargement of the pores, which enhanced the adsorption of RBV-5R dye [10,22,23].

3.1.3. *PSAC yield*

PSAC yield was found to decrease with increasing activation temperature, activation time and IR as shown in Figure 2. As expected, increase in activation temperature, time and IR would decrease the PSAC yield as a result of the intensifying dehydration, elimination reactions and the increased C–KOH and C–CO_2 reaction rate, which would release increasing volatiles, thereby resulting in a higher carbon burn off [17,18,23,24,25]. Indeed, the increase in activation temperature quickened the gasification reaction of carbon; therefore, the attack of the amorphous components which obstructed the pores caused a decrease in the carbon yield [10]. However, materials with higher carbon content would be volatilised to a much lesser extent and should undergo less weight loss [26]. A similar observation was reported by Hameed and co-workers in which the activated carbon yield for coconut husk-based and oil palm fibre-based activated carbons prepared using the same physiochemical activation method were also found to generally decrease with increasing activation temperature, activation time and IR [16,27,28].

3.2. *Process optimisation*

CCD has been used to optimise the parameters affecting RBV-5R dye removal and PSAC yield responses. In this case, it is difficult to optimise both responses because the interest region of factors is different. When RBV-5R dye removal increases, PSAC yield will decrease and vice versa [16]. Therefore, the function of desirability was applied using Design-Expert software (STAT-EASE Inc., Minneapolis, USA) in order to compromise between these responses [16]. In this optimisation analysis, the target criteria were set as maximum values for both responses, whereas the values of the variables were set in the range being studied. The predicted and experimental results of RBV-5R dye removal and PSAC yield obtained at optimum conditions are shown in Table 5. The optimum PSAC yield was obtained by using an activation temperature of 811 °C, activation time of 1.7 h and IR of 3.0. The optimum preparation condition of PSAC showed RBV-5R dye removal of 81.28% and PSAC yield of 28.18%. It was observed that the experimental values obtained were in good agreement with the values predicted from the models, with relatively small errors, which were only 2.81 and 3.44%, respectively for RBV-5R dye removal and PSAC yield.
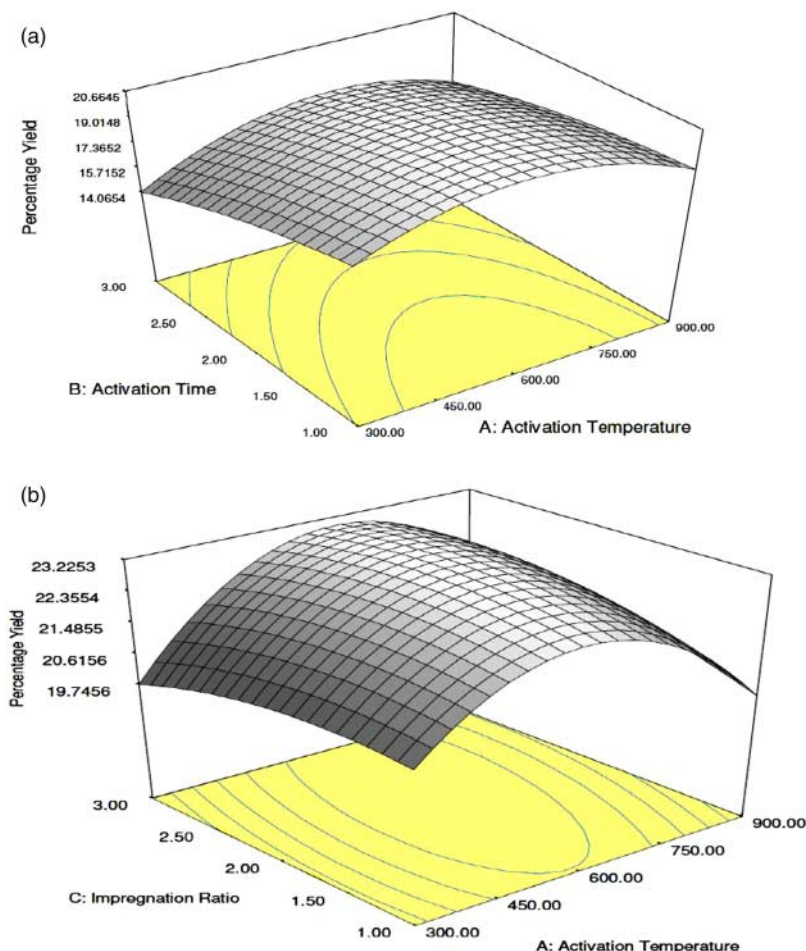
Figure 2. (a) Three-dimensional response surface plot of PSAC yield (effect of activation temperature and activation time, IR = 2.45). (b) Three-dimensional response surface plot of PSAC yield (effect of activation temperature and IR, $t = 2$ h).

Table 5. Model validation.

Model desirability	CO_2 activation temp (x_1) (°C)	CO_2 activation time (x_2) (h)	Impregnation ratio (x_3)	Y_1, RBV-5R removal (%)			Y_2, PSAC yield (%)		
				Pred.	Exp.	Error	Pred.	Exp.	Error
0.901	811	1.7	3.0	83.56	81.28	2.81	29.15	28.18	3.44

3.3. *Characterisation of PSAC*

3.3.1. *FTIR*

FTIR spectra of PSAC before and after adsorption are shown in Figure 3. In PSAC before adsorption spectrum (Figure 3a), the broad and intense absorption peaks at around $3412 \, cm^{-1}$ correspond to the O–H stretching vibrations due to inter- and intramolecular hydrogen bonding of polymeric
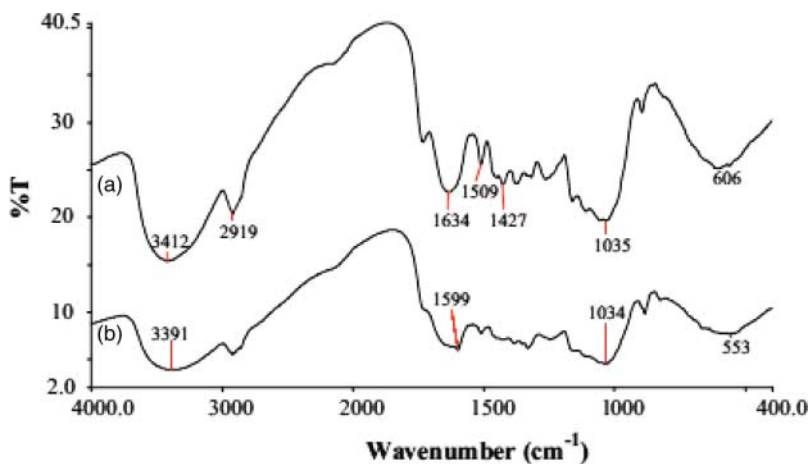
Figure 3. FTIR spectra of PSAC before and after adsorption.

compounds (macromolecular associations), such as alcohols, phenols and carboxylic acids, as in pectin, cellulose and lignin, thus showing the presence of 'free' hydroxyl groups on the PSAC surface. The peak at $2919\,cm^{-1}$ is attributed to the symmetric and asymmetric C–H stretching vibration of aliphatic acids. The peak at $1634\,cm^{-1}$ is due to asymmetric stretching vibrations of C=O and the peak observed at $1509\,cm^{-1}$ can be assigned to aromatic compound group. The other prominent peaks are due to NH_2, C=O and $-C-C-$ (1427, 1035 and $606\,cm^{-1}$, respectively) groups. After adsorption (Figure 3b), there is remarkable shift in positions of $-OH$, CO and $-C-C-$ group peaks to lower wave numbers indicating that RBV-5R dye binds mostly at $-OH$ and CO groups. The changes in FTIR spectra confirm the complexation of RBV-5R dye with the functional groups present in PSAC.

3.3.2. *BET*

It was found that the BET surface area, total pore volume and average pore diameter of PSAC were $1894\,m^2{\cdot}g^{-1}$, $1.107\,cm^3{\cdot}g^{-1}$ and 2.32 nm respectively. The porosity of PSAC is well developed with a higher surface area, total pore volume and larger average pore diameter, which are advantageous for dye adsorption. The average pore diameter of the PSAC was found to be 2.32 nm. This indicated that PSAC was mesoporous, with a relatively large surface area and total pore volume compared with commercially available activated carbons such as BDH from Merck, F100 and BPL from Calgon Corp. with BET surface areas of 1118, 957 and $972\,m^2{\cdot}g^{-1}$, as well as total pore volumes of 0.618, 0.526 and $0.525\,cm^3{\cdot}g^{-1}$, respectively [22].

3.3.3. *SEM*

Figure 4 shows the SEM images of (a) the raw PS and (b) the PSAC. Many large pores with a honeycomb shape were found on the surface of the PSAC, compared with the raw PS. This shows that the activation process was effective in creating well-developed pores on the surface of the precursor, leading to PSAC with large surface area and porous structure [29,30]. These pores allowed a good surface for RBV-5R reactive dye to be trapped and adsorbed [31].
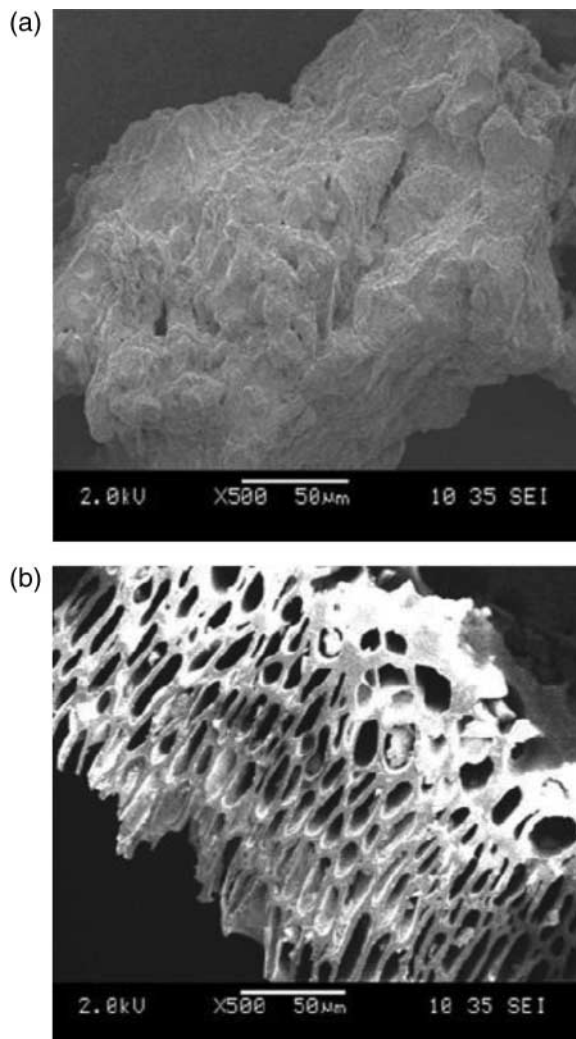
Figure 4.   SEM of raw PS and PSAC (magnification 500×).

Table 6.   Proximate analysis of PSAC.

Sample	Elemental analysis (%)				Proximate analysis (%)			
	C	H	N	$(O + S)^a$	Moisture	Volatile	Fixed carbon	Ash
Raw PS	35.46	4.17	0.52	59.85	13.14	52.35	30.26	4.25
PSAC	62.18	2.46	1.32	34.04	10.00	20.50	64.90	4.60

Note: [a]Estimated by difference.

3.3.4.   *Proximate and elemental analyses*

The proximate analyses of PSAC are presented in Table 6. The volatile matter and ash contents in the PSAC were 20.5 and 4.6% respectively. The fixed carbon content was satisfactory in the prepared activated carbon, having a value of 64.9%, indicating that the precursor was suitable in activated carbon preparation. For moisture content, it left ~10%. Elemental analyses of the raw

PS and prepared PSAC indicated that the percentages of C, H, N and others were 35.46, 4.17, 0.52 and 59.85 for the precursor and 62.18, 2.46, 1.32 and 34.04 for the activated carbon. The fixed carbon improved after activation, this is also noted in the elemental analysis. Both samples have a moderate nitrogen content, $<2\%$.

4. Conclusions

A CCD was conducted to study the effects of three activated carbon preparation variables: CO_2 activation temperature, CO_2 activation time and IR, on RBV-5R dye removal and PSAC yield. The optimal preparation conditions for PSAC were obtained using 811 °C activation temperature, 1.7 h activation time and 3.0 IR, resulting in 81.28% RBV-5R dye removal and 28.18% PSAC yield. The experimental values obtained for RBV-5R dye and PSAC were found to agree satisfactorily with the values predicted by the models, with deviation errors of 2.81 and 3.44%, respectively. Textural characterisation results revealed that the BET surface area of the PSAC prepared was 1894 $m^2 \cdot g^{-1}$, with total pore volume of 1.107 $cm^3 \cdot g^{-1}$ and average pore diameter of 2.32 nm indicating that the PSAC is mesoporous in nature. The PSAC produced demonstrated a large surface area and porous structure. The FTIR spectrum showed the presence of various functional groups on the surface of the activated carbon. PSAC was shown to be a promising low-cost material for the production of mesoporous activated carbon with high efficiency in removing RBV-5R dye from aqueous solutions.

References

[1] G. McKay and G.A. Sweeney, *Principles of dye removal from textile effluent*, Water Air Soil Pollut. 4 (1980), pp. 3–11.
[2] G. Palmieri, G. Cennamo, and G. Sannia, *Remazol Brilliant Blue R decolourisation by the fungus* Pleurotus ostreatus *and its oxidative enzymatic system*, Enzyme Microb. Technol. 36 (2005), pp. 17–24.
[3] H. Zollinger, *Colour Chemistry – Syntheses, Properties and Application of Organic Dyes and Pigments*, VCH, New York, 1987.
[4] V.M. Correia, T. Stephenson, and S.J. Judd, *Characterization of textile wastewaters, a review*, Environ. Technol. 15 (1994), pp. 917–919.
[5] G.B. Michaels and D.L. Lewis, *Sorption and toxicity of azo and triphenyl methane dyes to aquatic microbial population*, Environ. Toxicol. Chem. 4 (1985), pp. 45–50.
[6] T. Robinson, G. McMullan, R. Marchant, and P. Nigam, *Remediation of dyes in textile effluent, a critical review on current treatment technologies with a proposed alternative*, Bioresource Technol. 77 (2001), pp. 247–255.
[7] Z. Alam, S.A. Muyibi and J. Toramae, *Statistical optimization of adsorption processes for removal of 2,4-dichlorophenol by activated carbon derived from oil palm empty fruit bunches*, J. Environ. Sci. 19 (2007), pp. 674–677.
[8] F. Karacan, U. Ozden, and S. Karacan, *Optimization of manufacturing conditions for activated carbon from Turkish lignite by chemical activation using response surface methodology*, Appl. Therm. Eng. 27 (2007), pp. 1212–1218.
[9] R. Azargohar and A.K. Dalai, *Steam and KOH activation of biochar: experimental and modeling studies*, Micropor. Mesopor. Mater. 110 (2008), pp. 413–421.
[10] A. Baçaoui, A. Yaacoubi, A. Dahbi, C. Bennouna, R. Phan Tan Luu, F.J. Maldonado-Hodar, J. Rivera-Utrilla, and C. Moreno-Castilla, *Optimization of conditions for the preparation of activated carbons from olive-waste cakes*, Carbon 39 (2001), pp. 425–432.
[11] R. Azargohar and A.K. Dalai, *Production of activated carbon from Luscar char: experimental and modeling studies*, Micropor. Mesopor. Mater. 85 (2005), pp. 219–225.

[12] Z.R. Lazic, *Design of Experiments in Chemical Engineering*, 1st ed., Wiley-VCH Verlag, Weinheim, 2004.

[13] M.A. Ahmad and R. Alrozi, *Optimization of preparation conditions for mangosteen peel-based activated carbons for the removal of Remazol Brilliant Blue R using response surface methodology*, Chem. Eng. J. 165 (2010), pp. 883–890.

[14] D.C. Montgomery, *Design and Analysis of Experiments*, 7th ed., Wiley, New York, 2009.

[15] N.F. Zainudin, K.T. Lee, A.H. Kamaruddin, S. Bhatia, and A.R. Mohamed, *Study of adsorbent prepared from oil palm ash (OPA) for flue gas desulfurization*, Sep. Purif. Technol. 45 (2005), pp. 50–60.

[16] I.A.W. Tan, A.L. Ahmad, and B.H. Hameed, *Optimization of preparation conditions for activated carbons from coconut husk using response surface methodology*, Chem. Eng. J. 137 (2008), pp. 462–470.

[17] F.C. Wu and R.L. Tseng, *Preparation of highly porous carbon from fir wood by KOH etching and CO_2 gasification for adsorption of dyes and phenols from water*, J. Colloid Interface Sci. 294 (2006), pp. 21–30.

[18] D. Adinata, W.M.A. Wan Daud, and M.K. Aroua, *Preparation and characterization of activated carbon from palm shell by chemical activation with K_2CO_3*, Bioresource Technol. 98 (2007), pp. 145–149.

[19] A. Zabaniotou, G. Stavropoulos, and V. Skoulou, *Activated carbon from olive kernels in a two-stage process: industrial improvement*, Bioresource Technol. 99 (2008), pp. 320–326.

[20] Y. Sudaryanto, S.B. Hartono, W. Irawaty, H. Hindarso, and S. Ismadji, *High surface area activated carbon prepared from cassava peel by chemical activation*, Bioresource Technol. 97 (2006), pp. 734–739.

[21] M.K.B. Gratuito, T. Panyathanmaporn, R.A. Chumnanklang, N. Sirinuntawittaya, and A. Dutta, *Production of activated carbon from coconut shell: optimization using response surface methodology*, Bioresource Technol. 99 (2008), pp. 4887–4895.

[22] G.G. Stavropoulos and A.A. Zabaniotou, *Production and characterization of activated carbons from olive-seed waste residue*, Micropor. Mesopor. Mater. 82 (2005), pp. 79–85.

[23] A.C. Lua and T. Yang, *Effect of activation temperature on the textural and chemical properties of potassium hydroxide activated carbon prepared from pistachio nut shell*, J. Colloid Interface Sci. 274 (2004), pp. 594–601.

[24] C.Sentorun-Shalaby, M.G. Ucak-Astarlıoglu, L. Artok, and C. Sarıcı, *Preparation and characterization of activated carbons by one-step steam pyrolysis/activation from apricot stones*, Micropor. Mesopor. Mater. 88 (2006), pp. 126–134.

[25] T. Yang and A.C. Lua, *Characteristics of activated carbons prepared from pistachio nut shells by physical activation*, J. Colloid Interface Sci. 267 (2003), pp. 408–417.

[26] R.M. Suzuki, A.D. Andrade, J.C. Sousa, and M.C. Rollemberg, *Preparation and characterization of activated carbon from rice bran*, Bioresource Technol. 98 (2007), pp. 1985–1991.

[27] B.H. Hameed, I.A.W. Tan, and A.L. Ahmad, *Optimization of basic dye removal by oil palm fibre-based activated carbon using response surface methodology*, J. Hazard. Mater. 158 (2008), pp. 324–332.

[28] I.A.W. Tan, A.L. Ahmad, and B.H. Hameed, *Preparation of activated carbon from coconut husk: optimization study on removal of 2,4,6-trichlorophenol using response surface methodology*, J. Hazard. Mater. 153 (2008), pp. 709–717.

[29] P. Ricou-Hoeffer, I. Lecuyer and P.L. Cloirec, *Experimental design methodology applied to adsorption of metallic ions onto fly ash*, Water Res. 35 (2001), pp. 965–976.

[30] B.H. Hameed and F.B.M. Daud, *Adsorption studies of basic dye on activated carbon derived from agricultural waste:* Hevea brasiliensis *seed coat*, Chem. Eng. J. 139 (2008), pp. 48–55.

[31] N.K. Amin, *Removal of acid blue -106 dye from aqueous solution using new activated carbons developed from pomegranate peel: adsorption equilibrium and kinetics*, J. Hazard. Mater. 165 (2008), pp. 52–62.